

L. Carlen, H. A. Gustafsson, B. Jakobsson, T. Johansson, P. Kristiansson, O. B. Nielsen, A. Oskarsson, I. Otterlund, H. Ryde, B. Schröder, and G. Tibell, *Phys. Rev. C* **26**, 1299 (1982); M. Buenerd, in *Proceedings of the Twentieth Winter Meeting on Nuclear Physics*, Bormio, Italy, 1982 (unpublished).

⁴M. E. Brandan and A. Menchaca-Rocha, *Phys. Rev. C* **23**, 1272 (1981).

⁵H. G. Bohlen, M. R. Clover, G. Ingold, H. Lettau, and W. v. Oertzen, *Z. Phys. A* **308**, 121 (1982).

⁶H. Oeschler, H. L. Harney, D. L. Millis, and K. S. Sim, *Nucl. Phys. A* **325**, 463 (1979).

⁷J. Jaros, A. Wagner, L. Anderson, O. Chamberlain, R. Z. Fuzesy, J. Gallup, W. Gorn, L. Schroeder, S. Shannon, G. Shapiro, and H. Steiner, *Phys. Rev. C* **18**, 2273 (1978).

⁸T. J. Gooding, *Nucl. Phys.* **12**, 241 (1959).

⁹These scintillators were manufactured by Centre

d'Etudes Nucléaires de Saclay, S.T.I.P.E.

¹⁰R. G. Stokstad, R. M. Wieland, G. R. Satchler, C. B. Fulmer, D. C. Hensley, S. Raman, L. D. Rickertsen, A. H. Snell, and P. H. Stelson, *Phys. Rev. C* **20**, 655 (1979).

¹¹J. P. Wialeszko, private communication.

¹²J. Mougey, R. Ost, M. Buenerd, A. J. Cole, C. Guet, D. Lebrun, J. M. Loiseaux, P. Martin, M. Maurel, E. Monnard, H. Nifenecker, P. Perrin, J. Pinston, C. Ristori, P. de Saintignon, F. Schussler, L. Carlen, B. Jakobsson, A. Oskarsson, L. Otterlund, B. Schroeder, H. A. Gustafsson, T. Johansson, H. Ryde, J. P. Bondorf, O. B. Nielsen, and G. Tibell, *Phys. Lett.* **105B**, 25 (1981).

¹³R. M. DeVries, N. J. DiGiacomo, J. S. Kapustinski, J. C. Peng, W. E. Sondheim, J. W. Sunier, J. G. Cramer, R. E. Loveman, C. R. Gruhn, and H. H. Wieman, *Phys. Rev. C* **26**, 301 (1982).

Alpha-Particle Angular Distributions with Respect to Spin Direction

F. A. Dilmanian, D. G. Sarantites, M. Jääskeläinen,^(a) H. Puchta,^(b) and R. Woodward

Department of Chemistry, Washington University, St. Louis, Missouri 63130

and

J. R. Beene, D. C. Hensley, M. L. Halbert, and R. Novotny^(c)

Oak Ridge National Laboratory, Oak Ridge, Tennessee 37830

and

L. Adler, R. K. Choudhury, M. N. Namboodiri, R. P. Schmitt, and J. B. Natowitz

Cyclotron Institute and Department of Chemistry, Texas A & M University, College Station, Texas 77840

(Received 3 August 1982)

Angular distribution of alpha particles with respect to the spin direction of residual nuclei from fusion of 176-MeV ²⁰Ne with ¹⁵⁰Nd has been measured with the spin spectrometer. Below the Coulomb barrier, the ratio of the 90° to 0° yields with respect to spin direction increases with decreasing E_α . This effect is not shown by a statistical-model calculation using penetrabilities for spherical potentials, which suggests that the α -emitting nuclei are deformed with their longest axis perpendicular to the spin direction. If so, the deformation increases as the spin rises from ~ 34 to $64\hbar$.

PACS numbers: 21.10.Ft, 23.60.+e, 25.70.Fg, 27.70.+q

The shape and structure of the nucleus at high excitation and their evolution with spin are subjects of current interest. These properties of highly excited nuclei can be investigated by measurements of evaporated α particles.¹⁻³ We report here for the first time measurements of angular distributions of evaporated α particles with respect to spin direction, using the unique properties of the spin spectrometer.⁴⁻⁶ The spectrometer, a 4π γ -ray multidetector system, determines the magnitude and the orientation of the spin of the residual nuclei on an event-by-

event basis. This provides a sensitive method⁷ to investigate changes in nuclear shape as a function of spin.

A 176.6-MeV ²⁰Ne beam from the Oak Ridge isochronous cyclotron bombarded a 1.1-mg/cm² Nd target enriched to 96.1% in mass 150. The α particles were measured in nine Si surface-barrier $\Delta E, E$ telescopes, of which two were at 80° and one was at 90° to the beam ($\sim 89^\circ$ and 97° c.m.). The ΔE detectors had a thickness of 75 μm and an acceptance cone of $\sim 6^\circ$ half-angle. A Si detector at 8° identified evaporation residues

by their energy and flight time.

The spin spectrometer allows simultaneous measurement of the γ -ray multiplicity, M_γ , the total de-excitation energy, E^* , and the γ -ray angular correlations. In this experiment 70 of the 72 NaI detectors were used, covering 94.5% of the 4π sr. The spectrometer was triggered by any of the nine telescopes. For each event the NaI pulse heights and times, the particle pulse heights and times, and the cyclotron rf time were recorded on magnetic tape. The data collection procedure and the first steps in the analysis, including neutron- γ separation by time of flight, are described in Ref. 6.

The method used to determine the spin direction for each event is based on the fact that the γ cascades from rotational nuclei have a preponderance of stretched $E2$ transitions which exhibit a doughnutlike pattern about the spin axis [$W(\theta) = \frac{5}{4}(1 - \cos^4\theta)$]. The γ pattern for each event is projected on the plane perpendicular to the beam, under the assumption that the spin direction lies in that plane, and elaborate centroid-searching routines are used to find the angle φ specifying the short symmetry axis of the projected pattern. The uncertainty in the deduced spin direction of the evaporation residues (ER) comes from the finite multiplicity M_γ , the fraction of transitions in the cascade which are not stretched $E2$, the finite solid angle of the NaI detectors, the γ -ray scattering, the coincidence summing, and the neglect of the spin component along the beam direction. The aperture of the α detectors contributes to the uncertainty in the angle between the spin vector of ER and of the direction of the α particles. Furthermore, the loss of spin alignment due to nonstretched particle emission contributes to the uncertainty in the angle β between the spin, I , of the α -emitting nucleus and the direction of the α particle. All these effects were included in a Monte Carlo simulation to generate a spin response function $P(\beta, M_\gamma)$. Examples are given in Fig. 1(a) for $M_\gamma = 13$ (10 stretched $E2 + 3$ stretched dipole transitions) and $M_\gamma = 29$ (22 stretched $E2 + 7$ stretched dipole).

Spectra of α particles were obtained for five equal bins of 18° in φ and for the following five bins in the γ -ray coincidence fold, k : 11-14, 15-18, 19-22, 23-26, and 27-33. The k values were converted to M_γ and then to the ER spin values, I_{ER} , as described by Sarantites *et al.*⁸ These k bins correspond to I_{ER} ranges of ~14-29, 23-37, 32-44, 40-49, and 46-55. The average spins of the α -emitting nucleus that lead to the

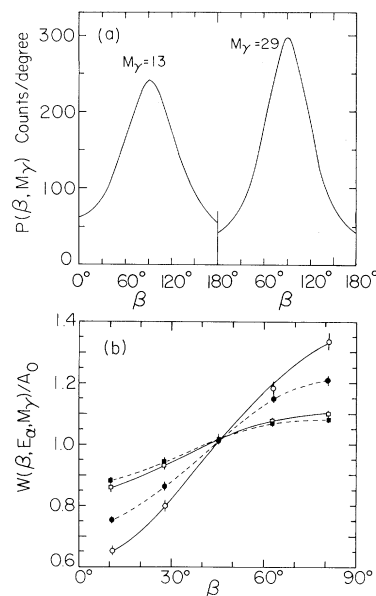


FIG. 1. (a) Examples of simulated spin response functions for finding the spin direction on an event-by-event basis. The initial spin was set at 90° . (b) Experimental angular distributions of α particles with respect to the spin direction. The open and closed squares correspond to $E_\alpha = 14$ and 21 MeV, respectively, for the $k = 11-14$ bin ($I \sim 34$). The open and closed circles correspond to $E_\alpha = 14$ and 21 MeV, respectively, for the $k = 23-26$ bin ($I \sim 59$). The solid and dashed lines give the least-squares fits of $A_0[1 + A_2P_2 + A_4P_4]$ to the data.

five k bins, calculated with the modified⁸ statistical-model code JULIAN-PACE,⁹ are ~34, 43, 51, 59, and 64, respectively. The k distributions for events gated with α particles only and those gated by α -ER coincidences are the same for $k \geq 10$, showing that contributions from processes such as deep inelastic scattering or fission are negligible. The experimental distribution of the spin direction φ associated with each telescope was transformed to the distributions in β in order to obtain $\langle\beta\rangle$ for each φ bin. The α -particle spectra were transformed to the center-of-mass system for $\alpha + {}^{166}\text{Er}$. Evaporation of several neutrons prior to α emission was found, on average, to have a negligible effect on the c.m. energy and angle. Comparison of the c.m. energy spectrum from the 80° and 150° telescopes indicates no significant nonequilibrium contribution for $E_\alpha \leq 27$ MeV.

Figure 2 shows examples of α -particle spectra at two angles relative to the spin direction. The angular distributions $W(\beta, E_\alpha, M_\gamma)$ for the three telescopes near 90° c.m. were fitted by

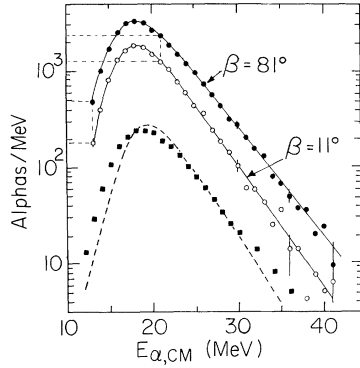


FIG. 2. Examples of α -particle energy spectra from the $k = 23$ –26 bin recorded in a telescope at 80° to the beam and corresponding to the angles of $\beta = 11^\circ$ and 81° with respect to the spin direction. The solid lines guide the eye. The dashed horizontal and vertical lines depict the difference in the anisotropies near and below the barrier. The experimental and calculated spectra integrated over k and β are shown in the lower part by the solid squares and the dashed curve, respectively.

$A_0[1 + A_2P_2(\cos\beta) + A_4P_4(\cos\beta)]$. Figure 1(b) shows some typical angular distributions and fits. The A_2 coefficients are shown in Fig. 3 as a function of E_α . The A_4 coefficients are essentially independent of E_α , with mean values -0.056 ± 0.006 , -0.036 ± 0.009 , -0.019 ± 0.012 , -0.015 ± 0.012 , and -0.012 ± 0.019 for the five k bins, respectively.

The α -particle angular distribution for initial spin I_i and final spin I_f can be expressed as

$$W_{E_\alpha, I_i, I_f}(\beta) = \sum_{\lambda} a_{E_\alpha, I_i, I_f, \lambda} B_{\lambda}(I_i) P_{\lambda}(\cos\beta), \quad (1)$$

where

$$a_{E_\alpha, I_i, I_f, \lambda} = \sum_i \frac{T_i(E_\alpha)}{\sum_i T_i(E_\alpha)} (-1)^{I_i + I_f} (2l + 1) \times (2I_i + 1)^{1/2} (2\lambda + 1)^{1/2} \begin{pmatrix} I_i & \lambda \\ 0 & 0 \end{pmatrix} \begin{Bmatrix} I_i & \lambda \\ I_f & I_f \end{Bmatrix}.$$

Here, $T_i(E_\alpha)$ are transmission coefficients, and $B_{\lambda}(I_i)$ is the statistical tensor describing the ensemble of spin orientations with respect to the quantization axis. In the present case the quantization axis is not fixed in space for all events but is instead chosen for each event to be the estimated spin direction. Thus $B_{\lambda}(I_i)$ describes the distribution of the true spin directions about this estimate. We obtain $B_{\lambda}(I_i)$ from the $P(\beta, M_\gamma)$, using the vector model to relate β to the magnetic substates of the spin. Angular distributions for comparison with experiment were calculated for various gates on E_α and M_γ by integrating Eq. (1) over distributions of $\Delta I = I_i - I_f$ obtained from the

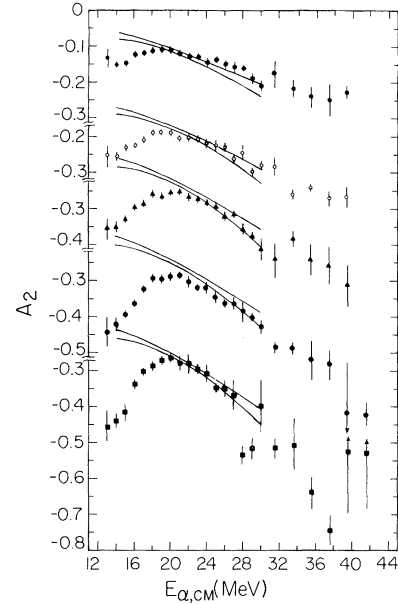


FIG. 3. A_2 coefficients as a function of E_α . The points represent experimental results. Closed and open circles correspond to k bins of 11–14 and 15–18 ($I \sim 34$ and 43), respectively. The closed triangles, closed large circles, and closed squares correspond to the k bins of 19–22, 23–26, and 27–32 ($I \sim 51, 59$, and 64), respectively. The pairs of curves are full width at half maximum boundaries for the calculated A_2 coefficients.

JULIAN-PACE simulation. The level-density parameter was taken as $A/9.5$ and yrast lines were taken from the rotating-liquid-drop model (RLDM)¹⁰; this choice of parameters reproduces the experimental cross sections¹¹ and the α energy spectra integrated over angle and spin (Fig. 2). In particular, the good agreement between the above-barrier slopes of the experimental and theoretical E_α spectra in Fig. 2 cannot be reproduced by level-density parameters $A/7.5$ and $A/10.5$. The agreement of the subbarrier slopes indicates that the $T_i(E_\alpha)$ coefficients used¹² are realistic [the $T_i(E_\alpha)$ coefficients used in Eq. (1) are the same used in the calculation with JULIAN-PACE].

The calculated A_2 coefficients agree well with the monotonic decrease of the experimental A_2 values above the Coulomb barrier (~ 21 MeV for a spherical nucleus), but do not reproduce the decrease of A_2 at low E_α (Fig. 3). The statistical-model results can be explained in the following terms. The α angular distribution is determined by the combined effect of the T_i and the level density. For a given E_α , T_i is constant up to some l and then decreases monotonically. The

level density favors transitions with large ΔI . As E_α increases, the T_l for larger l increase, leading to monotonically increasing anisotropy.

This general trend must be examined carefully for the (E_i^*, I_i) regions near the yrast line in the emitting nucleus, which in our calculation have a larger relative contribution to the subbarrier alpha emission. Here the scarcity of states accessible for small ΔI promotes low-energy alpha emission with fairly large ΔI and l in spite of small T_l values. This causes a decrease in slope of the calculated A_2 coefficients with decreasing E_α below the barrier as seen in Fig. 3. However, it cannot lead to the sharp downturn observed in the data, unless the level density behaves in a much different way from that assumed in the statistical code for energies as high as 30 MeV above the yrast line. The calculated contribution of emitting nuclei below such excitations for $E_\alpha \geq 14$ MeV is quite small. For example, the average excitation energy above the yrast line leading to $E_\alpha = 14.8$ MeV is 52 MeV. For this reason, pairing and shell effects are unlikely¹³ to be responsible for the entire effect.

A more appealing possibility to explain the dramatic decrease of the measured A_2 at low E_α is deformation of the emitting nucleus. This can be seen qualitatively from a simple geometrical picture of barrier penetration. If the lowest barrier (i.e., along the longest nuclear axis) happens to be at 90° to the spin, the subbarrier alpha particles will be emitted preferentially in that direction, while those above the barrier would not be much affected by the deformation. If this is the correct explanation of the deviation of the theory from the experiment, then the increase of this deviation with spin suggests that the deformation increases with spin.

Adopting the deformation interpretation, we can eliminate some combinations of shape and dominant collective motion on the basis of the preferred emission normal to the spin: An oblate spheroid rotating perpendicular to its symmetry axis and a prolate one rotating about its symmetry axis would be inconsistent with the data. Because of the high excitation energies of the α -emitting nuclei, it is natural to compare our results with the predictions of the RLDM.¹⁰ For a nucleus with $Z = 70$ and $A = 170$ the RLDM predicts a transition, starting at $I = 81$, from an oblate spheroid spinning about its symmetry axis to a triaxial shape rotating about its shortest axis. (The latter survives only up to $I \sim 84$ where the fission barrier vanishes.) Both of these con-

figurations are consistent with our results, but only the oblate shape is expected because $l_{cr} = 76$ for fusion in this system.¹⁴ A prolate nucleus rotating perpendicular to its symmetry axis is also consistent with our findings. Such a shape, however, could result from pairing and shell effects,¹⁵ which are unlikely to contribute except to the lowest two or three E_α bins. The RLDM prediction for the oblate deformation is $\epsilon \sim 0.1$ for the lowest k bin ($I \sim 34$) and $\epsilon \sim 0.3$ for the highest one ($I \sim 64$). Extraction of ϵ from the experimental data is a challenging, model-dependent problem, beyond the scope of this Letter.

In summary, we have measured angular distributions of evaporated α particles with respect to the spin direction by a new method. We have observed a large enhancement of anisotropy for subbarrier α particles. A reasonable interpretation is that the α -emitting nuclei are deformed with their longest axis at 90° to the spin direction and that their deformation increases with spin.

This work was supported in part by the U. S. Department of Energy. Oak Ridge National Laboratory is operated by Union Carbide Corporation under Contract No. W-7405-eng-26 with the U. S. Department of Energy. One of us (H.P.) thanks the Deutsche Forschungsgemeinschaft for a scholarship.

^(a)Present address: Department of Physics, University of Jyväskylä, Jyväskylä, Finland.

^(b)On leave from the Department of Physics, University of Munich, West Germany.

^(c)Present address: Department of Physics, University of Heidelberg, Heidelberg, West Germany.

¹J. R. Grover and J. Gilet, Phys. Rev. **157**, 823 (1967).

²M. A. McMahan and J. M. Alexander, Phys. Rev. C **21**, 1261 (1981).

³M. Blann and T. T. Komoto, Phys. Scr. **24**, 93 (1981).

⁴D. G. Sarantites *et al.*, Nucl. Instrum. Methods **171**, 503 (1980).

⁵D. G. Sarantites *et al.*, J. Phys. (Paris), Colloq. **41**, C10-269 (1980).

⁶M. Jääskeläinen *et al.*, to be published.

⁷L. Adler *et al.*, Bull. Am. Phys. Soc. **24**, 834 (1979).

⁸D. G. Sarantites *et al.*, Phys. Lett. **115B**, 441 (1982).

⁹Code JULIAN, M. Hillman and Y. Eyal, unpublished; modification PACE by A. Gavron, Phys. Rev. C **21**, 230 (1980).

¹⁰S. Cohen *et al.*, Ann. Phys. (N.Y.) **82**, 557 (1974).

¹¹D. G. Sarantites *et al.*, Phys. Rev. C **14**, 2138 (1976).

¹²J. R. Huizenga and G. Igo, Nucl. Phys. **29**, 462 (1972).

¹³A. V. Ignatyuk *et al.*, Nucl. Phys. **A346**, 191 (1980).

¹⁴M. L. Halbert *et al.*, Phys. Rev. C **17**, 155 (1978).

¹⁵A. Bohr and B. Mottelson, *Nuclear Structure* (Benjamin, New York, 1975), Vol. 2.